Title: Heterosynaptic Plasticity Determines the Set-Point for Cortical Excitatory-Inhibitory Balance

Authors: Rachel E. Field[1-4†], James A. D'amour[1-4†], Robin Tremblay[2,4,5], Christoph Miehl[6], Bernardo Rudy[2,4,5], Julijana Gjorgjieva[6,7], and Robert C. Froemke[1-4,8,9*]

Affiliations:

[1] Skirball Institute for Biomolecular Medicine,

[2] Neuroscience Institute,

[3] Department of Otolaryngology,

[4] Department of Neuroscience and Physiology,

[5] Department of Anesthesiology,

New York University School of Medicine, New York, NY, 10016, USA.

[6] Max Planck Institute for Brain Research, 60438 Frankfurt, Germany.

[7] School of Life Sciences, Technical University of Munich, 85354 Freising, Germany.

[8] Center for Neural Science,

New York University, New York, NY, 10003, USA.

[9] Howard Hughes Medical Institute Faculty Scholar

†: Co-first authorship

* To whom correspondence should be addressed:

Phone: 212-263-4082

Email: robert.froemke@med.nyu.edu

Abstract

Excitation in neural circuits must be carefully controlled by inhibition to regulate information processing and network excitability. During development, inhibitory and excitatory inputs in the cerebral cortex are initially mismatched but become co-tuned or 'balanced' with experience. However, little is known about the set-points for excitatory-inhibitory balance or the mechanisms for establishing or maintaining this balance. Here we show how coordinated long-term synaptic modifications calibrate populations of excitatory and inhibitory inputs onto mouse auditory cortical pyramidal neurons. Pairing pre- and postsynaptic activity induced plasticity at paired inputs and different forms of heterosynaptic plasticity at the strongest unpaired synapses, which required minutes of activity and dendritic Ca^{2+} signaling to be computed. Theoretical analyses demonstrated how the relative amount of heterosynaptic plasticity could normalize and stabilize synaptic strengths to achieve any possible excitatory-inhibitory correlation. Thus excitatory-inhibitory balance is dynamic and cell-specific, determined by distinct plasticity rules across multiple excitatory and inhibitory synapses.

One-Sentence Abstract

Heterosynaptic plasticity can rapidly and specifically balance inhibition with excitation across multiple inputs onto cortical pyramidal neurons.

In mature cortical networks and elsewhere throughout the adult nervous system, excitation is regulated by a complex set of inhibitory circuits. GABAergic inhibition is important in many features of nervous system function, including spike generation, dendritic integration, synaptic plasticity, sleep, learning and memory, and prevention of pathological activity such as epilepsy (1-5). Consequentially, inhibitory synapses must be calibrated to the relative strengths of excitatory synapses to ensure that neurons and networks are neither hypo- nor hyper-excitable for prolonged periods. In sensory cortex, this balance between excitation and inhibition seems to be established during early postnatal development (6-11). In particular, frequency tuning curves in the primary auditory cortex (AI) tend to be initially broad or erratic; excitatory inputs mature within the first 1-2 weeks of postnatal life in rodents, but inhibitory tuning requires auditory experience over weeks 2-4 to balance excitation (7,12,13). This balance is usually quantified in terms of the correlation between excitation and inhibition across a stimulus dimension such as visual orientation or sound frequencies, or the temporal correlation between the patterns of excitation and inhibition measured over time. Experimental studies have found that in most neurons even in mature circuits, these correlation values are not perfect (i.e., linear correlation coefficient r: 1.0) but instead are often distributed across a range centered around lower positive levels (r: 0.4-0.7). It is unclear if these observations indicate that it is difficult to maintain higher levels of balance in biological neural networks, or if instead the set-point at which excitation and inhibition are in equilibrium is actively maintained at this lower level.

Excitatory-inhibitory balance must also be dynamically maintained throughout life, as experience-dependent modification of excitatory synapses (e.g., occurring during and after development, learning, or conditioning) requires corresponding changes to inhibitory inputs (7,8,14). Network simulation studies supported by experimental data in vitro and in vivo indicate

that disruptions of excitatory-inhibitory balance can rapidly produce epileptiform activity and seizures within minutes (1,15-18), meaning that compensatory mechanisms must act quickly to re-stabilize neural circuits before pathological activity emerges. At least some of these compensatory or homeostatic adjustments take place over hours to days to retain overall cell excitability, as demonstrated in a variety of neural systems (19-22). It remains unclear if these processes would be able to correct for changes in excitability on the shorter time-scale of activity-dependent plasticity (seconds to minutes) in the input-specific manner required to preserve or promote differential neural computations. This may depend on different set-points for excitatory-inhibitory balance, based on the function of the neuron or neural circuit (e.g., single spike firing vs bursting, or narrowly vs broadly tuned for stimulus features).

An alternative for regulating overall excitability is heterosynaptic plasticity, defined as modifications to inputs not activated during induction of long-term potentiation (LTP) or other forms of long-term plasticity triggered at specific inputs (14,23-25). Heterosynaptic long-term modifications at specific subsets of monitored inputs have been observed after excitatory LTP at paired 'homosynaptic' sites (7,26-32). It is unknown whether inhibitory synapses also undergo heterosynaptic modifications or how these changes across multiple inputs might be coordinated to alter excitatory-inhibitory balance. Recently, we showed that spike-timing-dependent plasticity (STDP) could be induced at co-activated excitatory and inhibitory synapses (33). Spike pairing induced excitatory and inhibitory LTP, with the degree of inhibitory potentiation depending on the initial amplitude of co-evoked excitatory events. This naturally led to a normalization of the excitation-inhibition ratio at the paired inputs. Here we ask whether spike pairing also leads to heterosynaptic excitatory and inhibitory modifications, and if these changes might collectively reorganize or enhance the relationship between excitation and inhibition across inputs.

To examine how homosynaptic and heterosynaptic modifications might synergistically affect cortical excitatory-inhibitory balance, we made 129 whole-cell recordings from layer 5 pyramidal neurons in slices of mouse auditory cortex. An array of stimulation electrodes (inter-electrode spacing: 120 µm) was placed in layer 4 and used to sequentially evoke 4-8 sets of excitatory and inhibitory postsynaptic currents (EPSCs and IPSCs), each at a low presentation rate (0.033-0.2 Hz) recorded in voltage-clamp (**Fig. 1A**). This form of stimulation recruited separate populations of excitatory and inhibitory presynaptic inputs with a low degree of overlap across channels (**Fig. 1B, fig. S1**), in a manner that mimics the recruitment of thalamocortical inputs onto cortical neurons in vivo by sensory stimulation (34-37). After measuring baseline synaptic strength for 5-20 minutes, recordings were switched to current-clamp to pair synaptic inputs evoked by one channel of stimulation with postsynaptic spiking induced by brief depolarization through the whole-cell electrode (33,38,39). The other stimulation channels were not activated during pairing. Following pairing, we resumed sequential stimulation of all channels and monitored paired and unpaired EPSCs and IPSCs for at least 16-25 minutes after pairing.

We found that pairing presynaptic and postsynaptic activity could lead to long-term synaptic modifications at multiple inputs, including inputs that were not activated during the pairing procedure. While some of these changes could be variable from cell to cell, we consistently found that the strongest unpaired excitatory and inhibitory inputs (the 'original best' inputs) were specifically modified minutes after pairing. For example, in the recording shown in **Figure 1C**, repetitively pairing presynaptic activation of channel S4 with postsynaptic spiking (pre→post pairing) induced excitatory and inhibitory LTP at the paired channel (**Fig. 1C**, red symbols; EPSC amplitude indicated by filled circles increased by 39%, IPSC amplitude indicated by open circles increased by 51%). These forms of excitatory and inhibitory STDP are consistent with our previous

study (33). In contrast, the original best unpaired inputs (excitation evoked by channel S3 and inhibition evoked by S2) were both depressed (**Fig. 1C**, blue symbols; EPSCs decreased by –27%, IPSCs decreased by –72%). The other unpaired inputs were not substantially affected on average (**Fig. 1C**, black symbols). Thus spike pairing induces rapid and specific heterosynaptic modifications in addition to more conventional STDP at paired (homosynaptic) inputs.

These selective modifications to the paired and original best inputs acted together to reorganize the overall profile of excitation and inhibition (i.e., excitatory-inhibitory balance). As a metric of excitatory-inhibitory balance, we used the linear correlation coefficient r_{ei} of EPSCs and IPSCs evoked across stimulation channels. Linear correlation has previously been used to quantify excitatory-inhibitory balance in vivo (7,40-43) and in vitro (44,45). For this cell, the initial IPSC amplitudes evoked by each of the six channels were mostly unrelated to the strengths of excitation across the stimulation channels (**Fig. 1D**, left, r_{ei}-before: 0.25). This was unsurprising as, *a priori*, excitatory and inhibitory synapses activated by extracellular stimulation need not be functionally related despite spatial proximity near each electrode (in this recording, the original best EPSCs and IPSCs were evoked by different channels). After pairing, however, this correlation increased, and the amplitudes of EPSCs and IPSCs evoked by each stimulation site were more similar across all channels (**Fig. 1D**, right, r_{ei}-after: 0.48); i.e., when EPSCs were smaller, IPSCs tended to be smaller; conversely, when EPSCs were larger, IPSCs also tended to be larger. This was a consequence of coordinated homosynaptic and heterosynaptic modifications to the paired input (**Fig. 1D**, red arrow) and original best unpaired inputs (**Fig. 1D**, blue arrowheads). Such activity-dependent changes over multiple paired and unpaired synapses- which collectively act to improve excitatory-inhibitory balance- are similar to experience-dependent changes to excitatory and inhibitory synaptic tuning curves in young rodent auditory cortex in vivo (7).

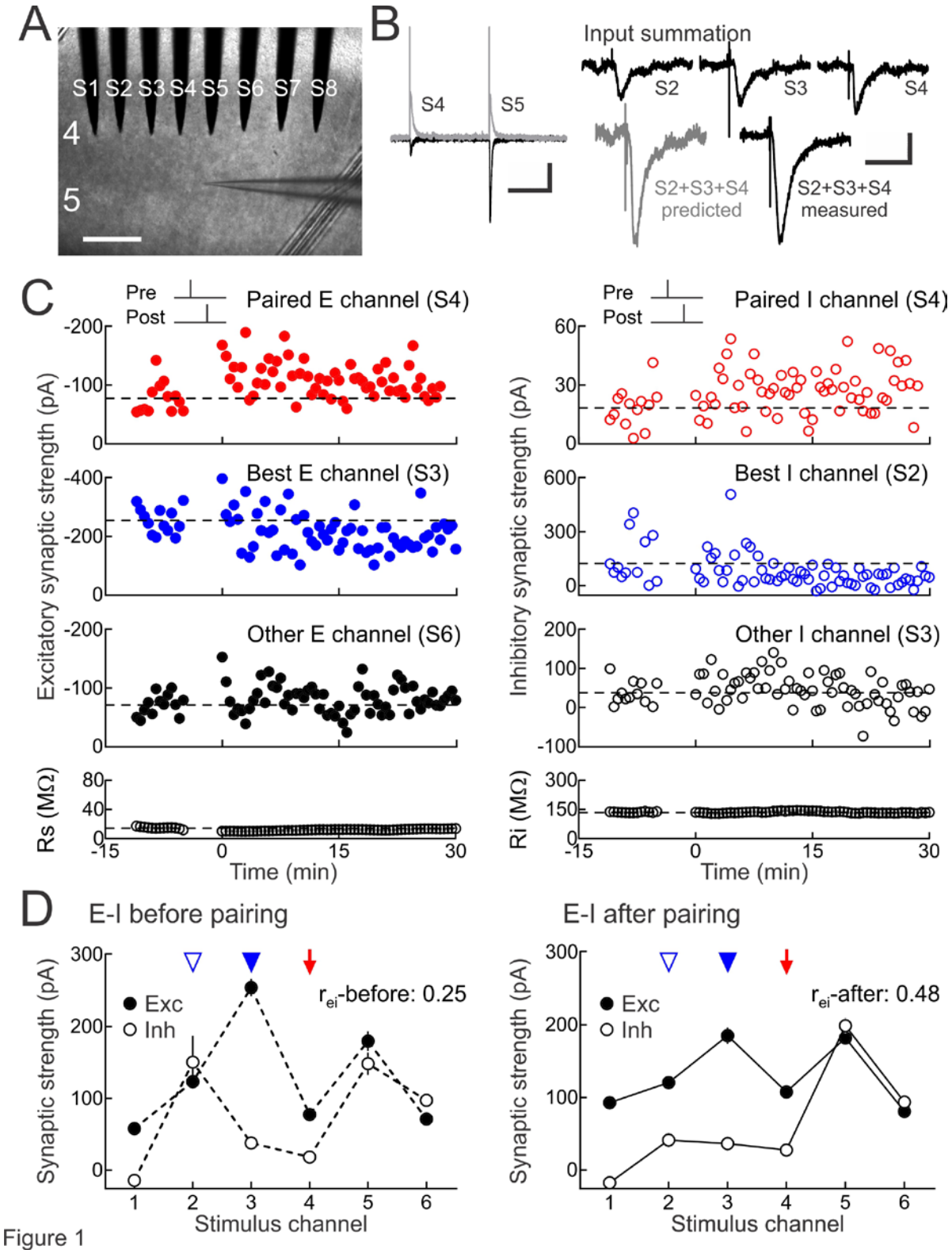

Figure 1

Figure 1. Spike pairing induces modifications of excitation and inhibition at paired and unpaired inputs.

(**A**) Whole-cell recordings from mouse auditory cortical layer 5 pyramidal cells in brain slices containing 8-electrode stimulation array (channels S1-S8) placed in layer 4. Scale, 250 µm.

(**B**) Left, recordings made in voltage-clamp to measure baseline and post-pairing EPSCs at −70 mV (black) and IPSCs at −30 mV (gray). Note that IPSC amplitudes do not necessarily scale with the amplitude of EPSCs evoked from the same channel. Scale: 500 msec, 200 pA. Pairing performed in current-clamp. Right, input summation testing, measuring inputs S3, S4, S5 separately and together; predicted summed response compared to measured summed response. Scale: 50 msec, 100 pA.

(**C**) Synaptic strength of multiple excitatory (left) and inhibitory inputs (right) onto the same neuron before and after pairing one channel with postsynaptic spiking. Top, example of excitatory and inhibitory plasticity induced by pre→post pairing at channel S4 (red, Δt: 0.5 msec; EPSCs before pairing: −77.4±7.4 pA; EPSCs after pairing: −107.5±6.1 pA, increase of 38.9%; IPSCs before pairing: 18.4±2.8 pA; IPSCs after pairing: 27.7±2.4 pA, increase of 50.6%). Dashed line, pre-pairing mean. Upper middle, heterosynaptic LTD at the strongest unpaired inputs onto this cell (blue, EPSCs at best channel S3 before: −254.0±12.3 pA, EPSCs after: −185.2±11.2 pA, decrease of −27.1%; IPSCs at best channel S2 before: 150.3±37.0 pA, IPSCs after: 41.4±10.1 pA, decrease of −72.4%). Lower middle, examples showing little change to other inputs (black, EPSCs at channel S6 before: −71.2±5.1 pA, EPSCs after: −80.7±6.9 pA, increase of 13.3%; IPSCs at channel S3 before: 37.9±8.2 pA, IPSCs after: 36.7±10.1 pA, decrease of −3.3%). Bottom, series and input resistances were stable (Rs before: 14.9±0.4 MΩ, Rs after: 12.4±0.1 MΩ, decrease of −16.2%; Ri before: 136.0±0.7 MΩ, Ri after: 134.6±0.8 MΩ, decrease of −1.0%).

(**D**) Improvement in excitatory-inhibitory balance after spike pairing at one channel; same cell as **C**. Excitatory-inhibitory correlation before pairing (r_{ei}-before, dashed lines) and after pairing (r_{ei}-after, solid lines). Spike pairing at a single channel led to long-lasting increase in excitatory-inhibitory correlation across all channels (r_{ei}-before: 0.25; r_{ei}-after: 0.48). Red arrow, paired channel. Blue arrowheads, original best excitation (filled) and inhibition (open). Error bars, SEM.

The relative timing of pre/postsynaptic spiking during pairing determined the sign of heterosynaptic plasticity at the original best inputs. In 25 recordings, we found that pre→post pairing reliably induced LTP at paired excitatory and inhibitory inputs with concomitant heterosynaptic LTD, which was reliably induced at the original best excitatory and inhibitory inputs (**Fig. 2A, fig. S2A, fig. S3A**). Across the other non-best unpaired inputs, we did not observe any systematic changes after pairing (**Fig. 2A**, bottom). In contrast, in 11 other recordings we observed that post→pre pairing induced excitatory LTD and inhibitory LTP at the paired inputs, as previously reported (33,39), together with heterosynaptic LTP at the original best excitatory and inhibitory inputs (**Fig. 2B, fig. S2B, fig. S3B**). As pre→post pairing potentiates paired inhibitory inputs, heterosynaptic inhibitory LTD provides a mechanism for bi-directional regulation of inhibitory synaptic strength. In contrast, heterosynaptic excitatory LTP might be useful for compensating for reductions in excitability after homosynaptic LTD at the paired excitatory input.

These coordinated synaptic modifications, induced by either pre→post or post→pre pairing, could affect overall excitatory-inhibitory correlation r_{ei} in similar ways. In general, when the correlation coefficient was initially low (r_{ei}-before <0.4), the correlation increased after pairing (**Fig. 2C, fig. S2**). This occurred for both pre→post and post→pre pairing (**Fig. 2C**, top; cells to left of red line at r=0.4 are almost all above the unity line), indicating that although the specific valence of synaptic modifications might be different, these changes act together to reorganize populations of synaptic inputs and enhance excitatory-inhibitory balance. However, when the excitatory-inhibitory correlation was initially high (r_{ei}-before >0.4), the correlation instead decreased after pairing (**Fig. 2C, fig. S3**). In the absence of postsynaptic spiking, no STDP was induced, and excitatory-inhibitory correlation was unchanged (**Fig. 2C**, bottom, gray 'No STDP').

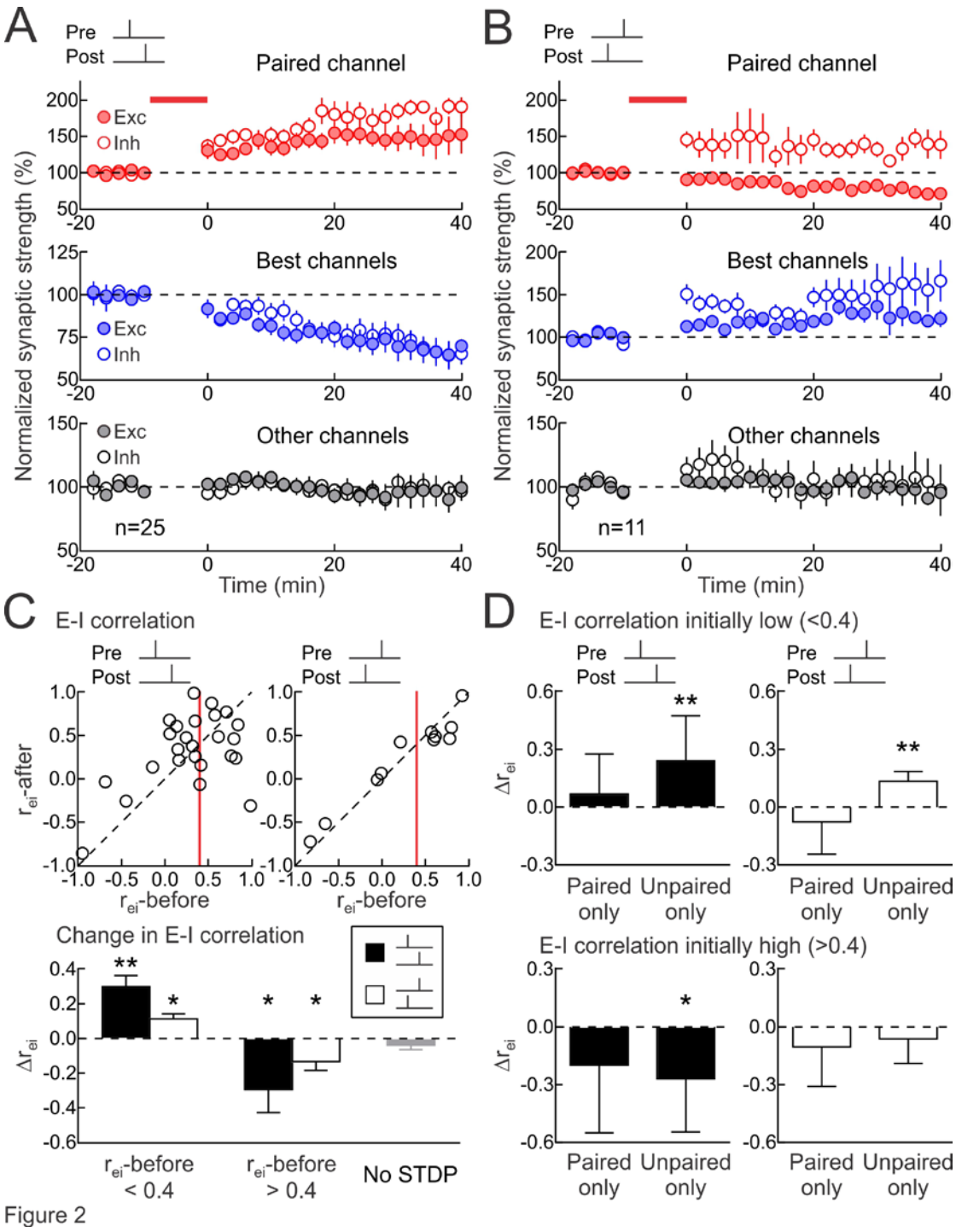

Figure 2

Figure 2. Heterosynaptic plasticity normalizes excitatory-inhibitory correlation.

(**A**) Summary of pre→post experiments on paired (top, red; paired EPSCs increased by 40.3±10.5% at 16-25 minutes post-pairing, n=25, p<0.0009, Student's paired two-tailed t-test, 18/25 cells showed significant excitatory LTP; paired IPSCs increased by 53.7±13.9%, p<0.0008, 19/25 cells showed significant inhibitory LTP), original best (middle, blue; originally-largest

EPSCs decreased by –21.7±4.1% at 16-25 minutes post-pairing, $p<10^{-4}$, 21/25 cells showed significant heterosynaptic excitatory LTD; originally-largest IPSCs decreased by –15.4±6.0%, p<0.02, 16/25 cells showed significant heterosynaptic inhibitory LTD), and other unpaired inputs (bottom, black; EPSCs increased by 1.4±8.0% at 16-25 minutes post-pairing, p>0.8; IPSCs increased by 0.7±4.6%, p>0.8). Filled symbols, excitation; open symbols, inhibition.

(**B**) Summary of post→pre pairing experiments on paired (top, red; paired EPSCs decreased by –17.0±6.4% at 16-25 minutes post-pairing, n=11, p<0.03, 9/11 cells showed significant excitatory LTD; paired IPSCs increased by 37.9±12.4%, p<0.02, 8/11 cells showed significant inhibitory LTP), original best (middle, blue; originally-largest EPSCs increased by 15.6±4.4% at 16-25 minutes post-pairing, p<0.006, 7/11 cells showed significant heterosynaptic excitatory LTP; originally-largest IPSCs increased by 25.1±8.6%, p<0.02, 7/11 cells showed significant heterosynaptic inhibitory LTP), and other unpaired inputs (bottom, black; EPSCs increased by 4.1±5.1% at 16-25 minutes post-pairing, p>0.4; IPSCs increased by 2.7±11.5%, p>0.8).

(**C**) Normalization of excitatory-inhibitory correlation after spike pairing. Top, excitatory-inhibitory correlation before (r_{ei}-before) and after (r_{ei}-after) pre→post pairing (left, n=25) or post→pre pairing (n=11). Red vertical line indicates r_{ei}:0.4. Bottom, changes in excitatory-inhibitory correlation after pairing (Δr_{ei}; when initially r<0.4 for pre→post pairing: 0.30±0.06, n=14, p<0.0005, post→pre pairing: 0.11±0.03, n=5, p<0.02; when initially r>0.4 for pre→post pairing: –0.29±0.13, n=11, p<0.05, post→pre pairing: –0.13±0.05, n=6, p<0.05; 'No STDP' controls without postsynaptic spiking: –0.04±0. 3, n=4, p>0.2; Student's paired two-tailed t-test).

(**D**) Heterosynaptic modifications to unpaired inputs were important for refining excitatory-inhibitory balance across channels. Considered separately, increases in synaptic strength only at paired synapses were less effective by themselves at normalizing excitatory-inhibitory correlation than changes to the remaining inputs ("Paired only", change in linear correlation coefficient Δr_{ei} when initially r<0.4 for pre→post pairing: 0.07±0.06, n=14, p>0.2, post→pre pairing: –0.08±0.08, n=5, p>0.3; and when initially r>0.4 for pre→post pairing: –0.20±0.11, n=11, p>0.1, post→pre pairing: –0.10±0.08, n=6, p>0.2; Student's paired two-tailed t-test; "Unpaired only", change in linear correlation coefficient Δr_{ei} when initially r<0.4 for pre→post pairing: 0.24±0.07, p<0.005, and for post→pre pairing: 0.13±0.02, p<0.005; and when initially r>0.4 for pre→post pairing: –0.27±0.09, p<0.02, but not for post→pre pairing: –0.06±0.05, p>0.2). *, p<0.05; **, p<0.01. Error bars, SEM.

Changes in excitatory-inhibitory correlation were due mainly to heterosynaptic modifications of unpaired inputs rather than homosynaptic plasticity of paired inputs, especially when the initial correlation was low. Considered independently, computing r_{ei}-after assuming only changes to paired inputs led to smaller correlation changes than only changes to unpaired inputs (**Fig. 2D**).

Thus pre/post spike pairing rapidly induces heterosynaptic plasticity to effectively normalize excitatory-inhibitory balance, adjusting the relation of inhibition to excitation to promote a moderate level of correlation of ~0.4. This value is close to that observed in rodent auditory cortex in vivo towards the end of the critical period for tonal frequency tuning (7), suggesting this value is a set-point that is actively maintained during this developmental stage of cortical organization. Intuitively, when the excitatory-inhibitory correlation was initially low, this was at least in part because the original best excitatory and inhibitory inputs were activated by different channels (in 12/14 pre→post and 5/5 post→pre pairing recordings). Heterosynaptic plasticity at the best excitatory and inhibitory inputs would naturally make those inputs more similar, since they were both depressed after pre→post pairing and potentiated after post→pre pairing. Note that when excitatory-inhibitory correlation was initially high, changes to the paired channel also served to normalize (in this case reducing) the correlation levels. This is expected for post→pre pairing, given that excitation and inhibition were modified in opposite directions. These findings indicate that single neurons have mechanisms for sensing and selectively modifying relative input strengths. In principle, these mechanisms could achieve nearly any degree of excitatory-inhibitory co-tuning. It may be computationally advantageous to not perfectly match excitation and inhibition, especially during postnatal developmental critical periods when cortical plasticity may be important for initializing sensory processing circuits.

To quantitatively assess this capacity in a theoretical framework, we simulated the effects of homosynaptic and heterosynaptic plasticity onto a model postsynaptic neuron driven by 12 excitatory and inhibitory inputs. We first considered a probabilistic model, where 50,000 excitatory and inhibitory tuning curves were generated randomly by sampling from a uniform distribution across channels (**Fig. 3A**, r_{ei}-before). This resulted in initial correlation r_{ei}-before values ranging from -0.9 to 0.9. One channel was chosen as the 'paired' channel, where excitation and inhibition were increased, and the original best excitatory and inhibitory channels were decreased by a fixed amount (**Fig. 3A**, r_{ei}-after). Following weight modification, we recomputed excitatory-inhibitory correlation r_{ei} across channels. As expected, the probability of r_{ei} correlation increasing or decreasing strongly depended on the initial correlation r_{ei}-before. Without heterosynaptic plasticity, the probability of r_{ei} increasing was higher than the probability of decreasing due to homosynaptic plasticity. However, with sufficiently strong heterosynaptic plasticity, a crossover occurred between the probability of r_{ei} increasing vs decreasing at an equilibrium point where excitatory-inhibitory correlation settled as increases and decreases of r_{ei} were themselves balanced (**Fig. 3B**). Correlation values initially higher than this set-point were likely to decrease, while correlation values initially lower were more likely to increase, as in the slice experiments (**Fig. 2C,D**). The most prominent influence on the updated correlation value (r_{ei}-after) to which the system converged was determined by the strength of heterosynaptic plasticity relative to homosynaptic plasticity, independent of the number of stimulus channels (**Fig. 3C**). The excitatory-inhibitory correlation equilibrium point (average r_{ei}-after) decreased as heterosynaptic plasticity strength was increased relative to homosynaptic plasticity strength. Thus, by titrating the relative strengths of heterosynaptic and homosynaptic plasticity, the system can in principle achieve any correlation value, i.e., an arbitrary set-point for stable excitatory-inhibitory balance.

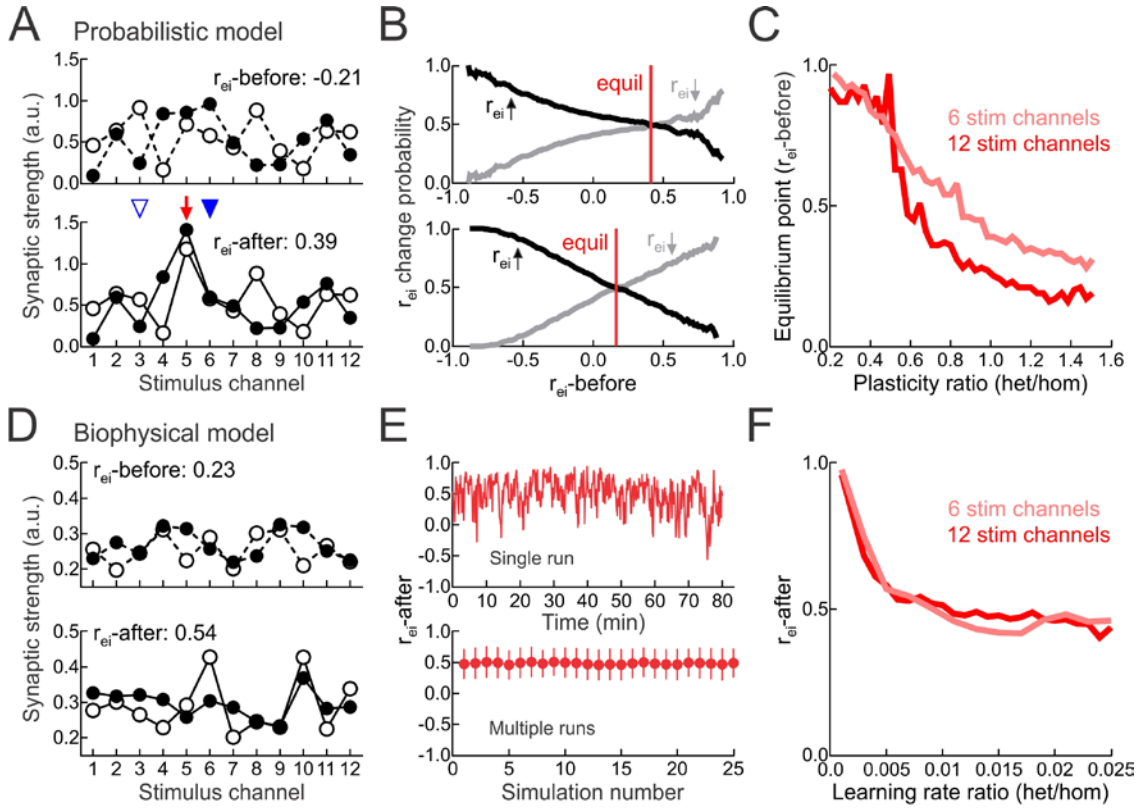

Figure 3

Figure 3. Heterosynaptic plasticity can determine the set-point for excitatory-inhibitory balance.

(**A**) Example tuning curves for probabilistic model of plasticity induction before and after synaptic weight adjustment.

(**B**) Results of all simulations, in terms of probability of r_{ei} increasing (black) or decreasing (gray) after plasticity, as a function of initial correlation. Where these lines cross at probability 0.5 is the equilibrium point ('equil') where homosynaptic and heterosynaptic plasticity balance each other and r_{ei} values would be expected to stabilize.

(**C**) r_{ei} equilibrium point for 6 (pink line) or 12 stimulation channels (red line) as a function of the ratio of heterosynaptic to homosynaptic plasticity.

(**D**) Example tuning curves for biophysical model of plasticity before and after simulation.

(**E**) Evolution of r_{ei} over time during a single simulation (top); and r_{ei}-after for 25 different tuning curve initializations (bottom). Ratio of heterosynaptic to homosynaptic plasticity was: $\frac{\eta^E_{het}}{\eta^E_w} = 1.3 * 10^{-2}$ ($\eta^E_{het} = 1.3 * 10^{-5}\, ms^{-1}$ and $\eta^I_{het} = 1.3 * 10^{-4}\, ms^{-1}$). Error bars indicate SEM.

(**F**) r_{ei}-after as function of excitatory heterosynaptic to homosynaptic learning rate ratio (η^E_{het}/η^E_w).

To determine whether this relationship between the excitatory-inhibitory correlation and the relative strengths of heterosynaptic vs. homosynaptic plasticity holds under more realistic conditions, we simulated a single postsynaptic integrate-and-fire neuron driven by 12 excitatory and inhibitory input channels. Each channel consisted of 10 excitatory and 10 inhibitory presynaptic conductance-based inputs, with weights modified by homosynaptic vs. heterosynaptic activity-dependent plasticity (**Fig. 3D, fig. S4A**). During the simulation, we made paired and unpaired channels fire at different rates to elicit postsynaptic spiking only during paired channel activation. Homosynaptic and heterosynaptic plasticity were implemented with biophysical traces that tracked pre- and postsynaptic activation online. As a consequence, r_{ei} fluctuated around a constant mean (**Fig. 3E**, top), which was consistent across different initial conditions (**Fig. 3E**, bottom). Similar to the probabilistic model (**Fig. 3A-C**), the excitatory-inhibitory correlation converged to a value that depended on the relative learning rates of heterosynaptic vs. homosynaptic plasticity (**Fig. 3F**). In particular, when homosynaptic plasticity was dominant, r_{ei} was high and the excitatory and inhibitory weights gradually increased over the simulation. In contrast, when heterosynaptic plasticity was dominant, r_{ei} was low and the excitatory and inhibitory weights during training gradually decreased. When the strengths of homosynaptic and heterosynaptic plasticity were approximately balanced, the excitatory and inhibitory weights were relatively stable during an extended period of training (**fig. S4B**) and r_{ei}-after converged to the value of 0.45-0.5, close to the values observed experimentally. These simulations demonstrate that heterosynaptic plasticity can powerfully control the positive feedback of homosynaptic plasticity, compensating for this process to achieve nearly any relation between excitatory and inhibitory tuning curves simply by adjusting the strength relative to homosynaptic plasticity.

We next examined the biological mechanisms that might enable heterosynaptic plasticity to occur selectively at the original best unpaired inputs. We first used two-photon Ca^{2+} imaging to examine dendritic Ca^{2+} events in layer 5 pyramidal cells during spike pairing (**fig. S5A**). We found that both pre→post and post→pre pairing led to a broadening of backpropagating action potential-evoked Ca^{2+} transients (**fig. S5B,C**; 'Normal solution'). We wondered if this enhanced Ca^{2+} signaling triggered by spike pairing was related to the phenomenon of Ca^{2+}-induced Ca^{2+} release from internal stores (46,47). This mechanism could potentially provide a means for intracellular communication across multiple synapses and has been implicated in heterosynaptic modifications in other temporal lobe structures, including amygdala (30) and hippocampus (48). We found that intracellular perfusion with thapsigargin (to deplete internal calcium stores, 10 μM) prevented this broadening of the Ca^{2+} event, such that transients evoked during pre→post and post→pre pairing were no different than Ca^{2+} transients triggered by postsynaptic spikes alone (**fig. S5B,C**; 'Thapsigargin').

Ca^{2+}-induced Ca^{2+} release was also the major mechanism for heterosynaptic plasticity (**fig. S6**). Either intracellular thapsigargin (10 μM, **fig. S6A,E**) or ruthenium red (which blocks Ca^{2+} release from internal stores, 20 μM; **fig. S6D, fig. S7**) prevented heterosynaptic modifications but spared changes to paired excitatory and inhibitory inputs after pre→post or post→pre pairing, which were comparable to the magnitudes of those forms of plasticity under normal recording conditions (**fig. S6B**). In contrast, bath application of APV (50 μM) to block NMDA receptors (**fig. S6C**) prevented all changes to paired and unpaired excitatory and inhibitory inputs. Therefore, the intracellular calcium signaling initiated by activation of NMDA receptors at paired excitatory synapses subsequently triggered a set of other modifications, mainly to paired inhibitory synapses and the original best unpaired excitatory and inhibitory synapses.

These results show that heterosynaptic plasticity can be selectively induced at a specific subset of excitatory and inhibitory inputs onto individual postsynaptic neurons. The original best inputs are necessarily locally but not globally maximal, as only a fraction of the total inputs received by these neurons were activated by the stimulation electrode array. As heterosynaptic changes were expressed ~10-20 minutes after pairing, we hypothesized that these locally-maximal inputs were computed by postsynaptic cells within this brief post-pairing period. To test this prediction, we performed a final set of experiments in which multiple inputs were monitored before and after pre→post or post→pre pairing, as before; however, for ten minutes immediately following pairing, the original best excitatory and inhibitory inputs (selected to be on the same input channel) were not stimulated.

We found that during this ten-minute period, the second-largest inputs ('relative best' inputs) were selectively affected by heterosynaptic modifications rather than the original best inputs. In the recording shown in **Figure 4A**, channel 8 evoked the originally-largest EPSCs and IPSCs, channel 6 evoked the second-largest EPSCs and IPSCs, and channel 4 was the paired channel. After pre→post pairing, channel 8 was turned off for ten minutes. During that period, the paired EPSCs and IPSCs increased, while heterosynaptic LTD was induced at the 'relative best' EPSCs and IPSCs evoked by channel 6. When channel 8 was reactivated, the EPSCs and IPSCs at that channel remained at their initial amplitudes and were stable until the end of the recording. Over all recordings, the relative best input during the ten-minute post-pairing period was selectively affected by heterosynaptic modifications rather than the original best inputs (**Fig. 4B**). Similarly, when the original best input was not presented after post→pre pairing, the relative best input instead experienced heterosynaptic plasticity; in this case, heterosynaptic LTP of both excitation and inhibition (**fig. S8**).

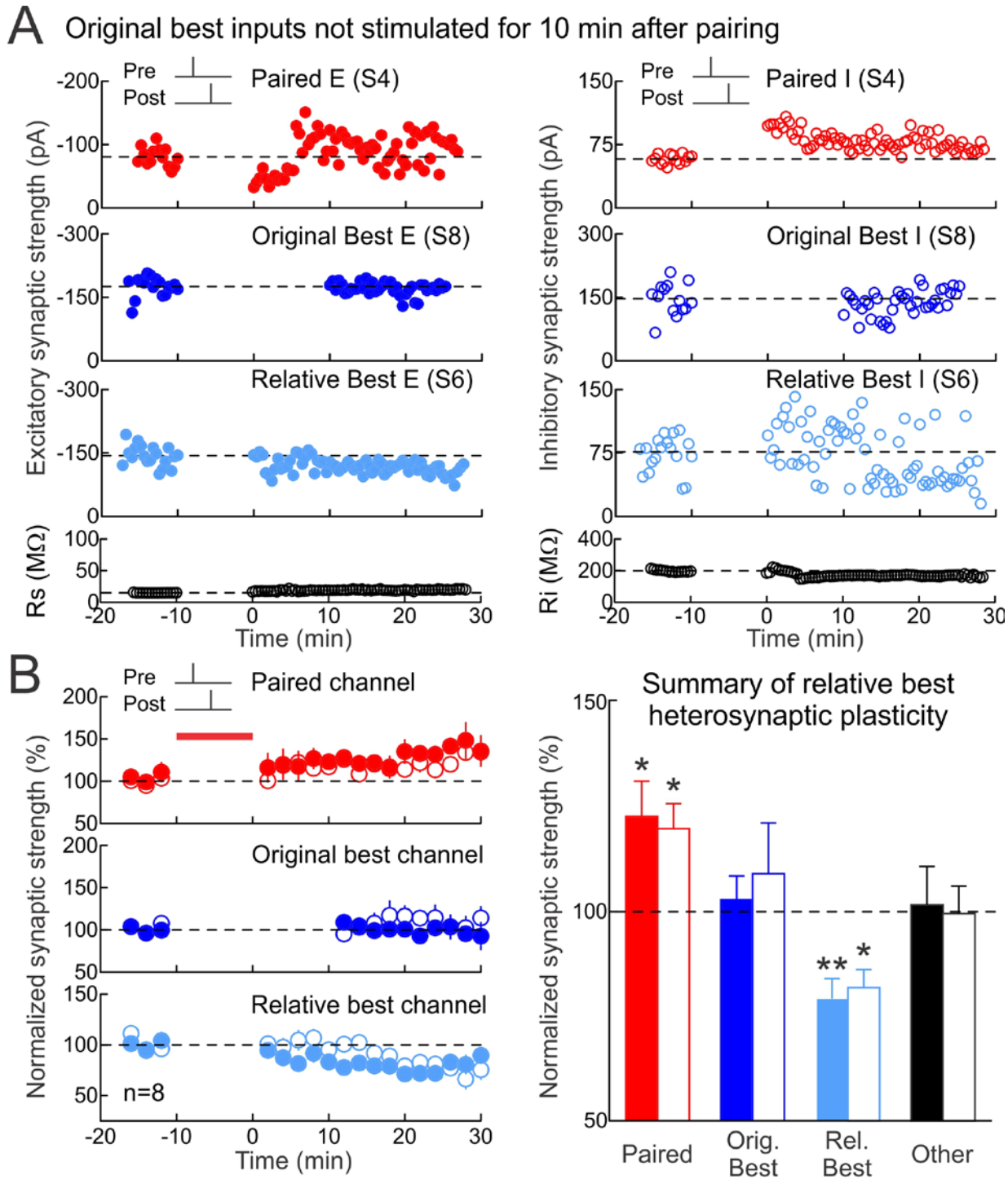

Figure 4

Figure 4. Postsynaptic neurons compute maximally strong inputs for heterosynaptic plasticity in a ten-minute period following induction of homosynaptic modifications.

(**A**) Deactivating original best input channel led to heterosynaptic excitatory and inhibitory LTD at the second best ('relative best') channel after pre→post pairing. Top, example of excitatory LTP (left) and inhibitory LTP (right) induced by pre→post pairing at channel S4 (red, Δt=4 msec; EPSCs before pairing: –80.7±3.9 pA, EPSCs after pairing: –90.7±4.7 pA, increase of 12.4%; IPSCs before pairing: 58.0±1.4 pA, IPSCs after pairing: 77.0±1.7 pA, increase of 32.9%). Dashed line, pre-pairing mean. Upper middle, original best inputs evoked by S8 were unaltered when this channel was turned off for ten minutes immediately after pairing (dark blue, original best EPSCs before: –175.6±5.7 pA, original best EPSCs after: –168.6±3.1 pA, decrease of –4.0%; original best IPSCs before: 146.3±10.1 pA, original best IPSCs after: 146.8±5.2 pA, increase of 1.0%). Lower middle, heterosynaptic depression was induced at the relative best inputs evoked by S6 (light blue, relative best EPSCs before: –143.6±5.6 pA, relative best EPSCs after: –114.4±2.5 pA, decrease of –20.3%; relative best IPSCs before: 73.7±5.0 pA, relative best IPSCs after: 52.9±5.4 pA, decrease of –28.3%). Bottom, series and input resistance (Rs before: 15.1±0.1 MΩ, Rs after: 19.5±0.2 MΩ, increase of 28.7%; Ri before: 199.2±1.9 MΩ, Ri after: 169.6±0.7 MΩ, decrease of –14.8%).

(**B**) Summary of pre→post experiments with original best input channel deactivated for the ten-minute after-pairing period. Shown are changes to paired inputs (red; paired EPSCs increased by 22.7±8.4% at 16-25 minutes post-pairing, n=8, $p<0.04$, Student's paired two-tailed t-test; paired IPSCs increased by 19.8±6.0%, $p<0.02$), original best inputs (dark blue; originally-largest EPSCs increased by 2.8±5.6% at 16-25 minutes post-pairing, $p>0.6$; originally-largest IPSCs increased by 9.0±12.1%, $p>0.4$), relative best inputs (light blue; EPSCs decreased by –20.6±4.8% at 16-25 minutes post-pairing, $p<0.004$; IPSCs decreased by –18.2±4.4%, $p<0.02$), and averaged other inputs (black; EPSCs increased by 1.6±9.2% at 16-25 minutes post-pairing, $p>0.8$; IPSCs decreased by –0.5±6.6%, $p>0.9$). Filled symbols, excitation; open symbols, inhibition. Left, time course (compare with **Fig. 2A**); right, summary of changes at 16-25 minutes after pairing.

This experiment demonstrates that heterosynaptic plasticity can be specifically manipulated, such that these changes selectively occur at whichever inputs were most strongly activated in a restricted post-pairing period. Furthermore, these results show that cortical neurons have a Ca^{2+}-dependent mechanism for determining and adjusting overall excitation and excitatory-inhibitory balance in a rapid and stimulus-specific manner.

Here we have described how organized forms of long-term homosynaptic and heterosynaptic plasticity selectively adjust populations of synaptic inputs onto mouse cortical pyramidal neurons to achieve a particular set-point for excitatory-inhibitory balance. Although inputs evoked by each stimulation channel may not initially be functionally related, these inputs become bound together via repetitive co-activation together with postsynaptic spiking. This might emulate how novel sensory stimuli recruit initially-unrelated inputs, which become functionally coupled via mechanisms of experience-dependent plasticity. Part of this mechanism involves computing local maxima of incoming inputs for selective modifications of specific synapses. Combined with slower forms of homeostatic plasticity (22), individual cortical neurons have the capability to integrate or accumulate recent activity over minutes to hours, enabling flexible representations of external stimuli and control over excitability on multiple short and long time-scales.

Although excitatory-inhibitory balance is a fundamental feature of neural networks (10,14,40,45), it has remained unclear how this organization is set up and calibrated on-line, especially in response to changes of excitatory synapses believed to be important for learning and memory storage. Instead of a slower global optimization process- which might be difficult to implement biologically- our results demonstrate that a restricted set of activity-dependent changes is sufficient to normalize excitatory-inhibitory balance within minutes, enhancing the relation

between inhibition and excitation when mismatched, or reducing this value if inhibition is too restrictive. Our theoretical analysis indicates that the definition of excitatory-inhibitory balance can be dynamic, and this set-point is determined by the relative degree to which heterosynaptic modifications are engaged. Consequentially, heterosynaptic plasticity and inhibitory plasticity work together to automatically restructure cortical circuits after induction of long-term excitatory modifications, to update information storage and enable flexible computation without disrupting overall network function.

References and Notes

1. Cossart, R., Dinocourt, C., Hirsch, J.C., Merchan-Perez, A., De Felipe, J., Ben-Ari, Y., Esclapez, M., and Bernard, C. (2001). Dendritic but not somatic GABAergic inhibition is decreased in experimental epilepsy. Nat. Neurosci. *4*, 52-62.
2. Isaacson, J.S., and Scanziani, M. (2011). How inhibition shapes cortical activity. Neuron *72*, 231-243.
3. Oliveira, M.S., Pacheco, L.F., Mello, C.F., Cavalheiro, E.A., and Garrido-Sanabria, E.R. (2011). Epileptiform activity in the limbic system. Front. Biosci. *3*, 565-593.
4. Scharfman, H.E., and Brooks-Kayal, A.R. (2014). Is plasticity of GABAergic mechanisms relevant to epileptogenesis? Adv. Exp. Med. Biol. *813*, 133-150.
5. Hattori, R., Kuchibhotla, K., Froemke, R.C., and Komiyama, T. (2017). Modulation and plasticity of inhibition. Nat. Neurosci. *20*, 1199-1208.
6. Gandhi, S.P., Yanagawa, Y., and Stryker, M.P. (2008). Delayed plasticity of inhibitory neurons in developing visual cortex. Proc. Natl. Acad. Sci. U S A. *105*, 16797-16802.
7. Dorrn, A.L., Yuan, K., Barker, A.J., Schreiner, C.E., and Froemke, R.C. (2010). Developmental sensory experience balances cortical excitation and inhibition. Nature *465*, 932-936.
8. House, D.R.C., Elstrott, J., Koh, E., Chung, J., and Feldman, D.E. (2011). Parallel regulation of feedforward inhibition and excitation during whisker map plasticity. Neuron *72*, 819-831.
9. Kuhlman, S.J., Olivas, N.D., Tring, E., Ikrar, T., Xu, X., and Trachtenberg, J.T. (2013). A disinhibitory microcircuit initiates critical-period plasticity in the visual cortex. Nature *501*, 543-546.
10. Takesian, A.E., and Hensch, T.K. (2013). Balancing plasticity/stability across brain development. Prog Brain Res. *207*, 3-34.

11. Cai, D., *et al*. (2017). A critical role of inhibition in temporal processing maturation in the primary auditory cortex. Cereb. Cortex in press.
12. Chang, E.F., Bao, S., Imaizumi, K., Schreiner, C.E., and Merzenich, M.M. (2005). Development of spectral and temporal response selectivity in the auditory cortex. Proc. Natl. Acad. Sci. U.S.A. *102*, 16460-16465.
13. de Villers-Sidani, E., Chang, E.F., Bao, S., and Merzenich, M.M. (2007). Critical period window for spectral tuning defined in the primary auditory cortex (A1) in the rat. J. Neurosci. *27*, 180-189.
14. Froemke, R.C. (2015). Plasticity of cortical excitatory-inhibitory balance. Annu. Rev. Neurosci. *38*, 195-219.
15. Toader, O., Forte, N., Orlando, M., Ferrea, E., Raimondi, A., Baldelli, P., Benfenati, F., and Medrihan, L. (2013). Dentate gyrus network dysfunctions precede the symptomatic phase in a genetic mouse model of seizures. Front. Cell. Neurosci. *7*, 138.
16. Ren, H., Shi, Y.J., Lu, Q.C., Liang, P.J., and Zhang, P.M. (2014). The role of the entorhinal cortex in epileptiform activities of the hippocampus. Theor. Biol. Med. Model. *11*, 14.
17. Avoli, M., de Curtis, M., Gnatkovsky, V., Gotman, J., Köhling, R., Lévesque, M., Manseau, F., Shiri, Z., and Williams, S. (2016). Specific imbalance of excitatory/inhibitory signaling establishes seizure onset pattern in temporal lobe epilepsy. J. Neurophysiol. *115*, 3229-3237.
18. Dehghani, N., Peyrache, A., Telenczuk, B., Le Van Quyen, M., Halgren, E., Cash, S.S., Hatsopoulos, N.G., and Destexhe, A. (2016). Dynamic balance of excitation and inhibition in human and monkey neocortex. Sci. Rep. *6*, 23176.
19. Lissin, D.V., Gomperts, S.N., Carroll, R.C., Christine, C.W., Kalman, D., Kitamura, M., Hardy, S., Nicoll, R.A., Malenka, R.C., and von Zastrow, M. (1998). Activity differentially

regulates the surface expression of synaptic AMPA and NMDA glutamate receptors. Proc. Natl. Acad. Sci. U S A *95*, 7097-7102.

20. Turrigiano, G.G., Leslie, K.R., Desai, N.S., Rutherford, L.C., and Nelson, S.B. (1998). Activity-dependent scaling of quantal amplitude in neocortical neurons. Nature *391*, 892-896.
21. Thiagarajan, T.C., Lindskog, M., and Tsien, R.W. (2005). Adaptation to synaptic inactivity in hippocampal neurons. Neuron *47*, 725-737.
22. Turrigiano, G.G. (2008) The self-tuning neuron: synaptic scaling of excitatory synapses. Cell 135, 422-435.
23. Chistiakova, M., Bannon, N.M., Chen, J.Y., Bazhenov, M., and Volgushev, M. (2015). Homeostatic role of heterosynaptic plasticity: models and experiments. Front. Comput. Neurosci. *9*, 89.
24. Hiratani, N., and Fukai, T. (2017). Detailed dendritic excitatory/inhibitory balance through heterosynaptic spike-timing-dependent plasticity. J. Neurosci. *37*, 12106-12122.
25. Zenke, F., Gerstner, W., and Ganguli, S. (2017). The temporal paradox of Hebbian learning and homeostatic plasticity. Curr. Opin. Neurobiol. *43*, 166-176.
26. Lynch, G.S., Dunwiddie, T., and Gribkoff, V. (1977). Heterosynaptic depression: a postsynaptic correlate of long-term potentiation. Nature *266*, 737-739.
27. Christie, B.R., and Abraham, W.C. (1992). NMDA-dependent heterosynaptic long-term depression in the dentate gyrus of anaesthetized rats. Synapse *10*, 1-6.
28. Muller, D., Hefft, S., and Figurov, A. (1995). Heterosynaptic interactions between LTP and LTD in CA1 hippocampal slices. Neuron *14*, 599-605.
29. Scanziani, M., Malenka, R.C., and Nicoll, R.A. (1997). Role of intercellular interactions in heterosynaptic long-term depression. Nature *380*, 446-450.

30. Royer, S., and Pare, D. (2003). Conservation of total synaptic weight through balanced synaptic potentiation and depression. Nature *422*, 518-522.

31. Froemke, R.C., Carcea, I., Barker, A.J., Yuan, K., Seybold, B.A., Martins, A.R., Zaika, N., Bernstein, H., Wachs, M., Levis, P.A., Polley, D.B., Merzenich, M.M., and Schreiner, C.E. (2013). Long-term modification of cortical synapses improves sensory perception. Nat. Neurosci. *16*, 79-88.

32. Basu, J., Zaremba, J.D., Cheung, S.K., Hitti, F.L., Zemelman, B.V., Losonczy, A., and Siegelbaum, S.A. (2016). Gating of hippocampal activity, plasticity, and memory by entorhinal cortex long-range inhibition. Science *351*, aaa5694.

33. D'amour, J.A., and Froemke, R.C. (2015). Inhibitory and excitatory spike-timing-dependent plasticity in the auditory cortex. Neuron *86*, 514-528.

34. Miller, L.M., Escabí, M.A., Read, H.L., and Schreiner, C.E. (2001). Functional convergence of response properties in the auditory thalamocortical system. Neuron *32*, 151-160.

35. Lee, C.C., Imaizumi, K., Schreiner, C.E., and Winer, J.A. (2004). Concurrent tonotopic processing streams in auditory cortex. Cereb. Cortex *14*, 441-451.

36. Froemke, R.C., Merzenich, M.M., and Schreiner, C.E. (2007). A synaptic memory trace for cortical receptive field plasticity. Nature *450*, 425-429.

37. Hackett, T.A., Barkat, T.R., O'Brien, B.M., Hensch, T.K., and Polley, D.B. Linking topography to tonotopy in the mouse auditory thalamocortical circuit. J. Neurosci. *31*, 2983-2995.

38. Bi, G.Q., and Poo, M.M. (1998). Synaptic modifications in cultured hippocampal neurons: dependence on spike timing, synaptic strength, and postsynaptic cell type. J. Neurosci. *18*, 10464-10472.

39. Feldman, D.E. (2000). Timing-based LTP and LTD at vertical inputs to layer II/III pyramidal cells in rat barrel cortex. Neuron *27*, 45-56.

40. Wehr, M. and Zador, A. M. (2003). Balanced inhibition underlies tuning and sharpens spike timing in auditory cortex. Nature *426*, 442-446.

41. Higley, M.J., and Contreras, D. (2006). Balanced excitation and inhibition determine spike timing during frequency adaptation. J. Neurosci. *26*, 448-457.

42. Okun, M., and Lampl, I. (2008). Instantaneous correlation of excitation and inhibition during ongoing and sensory-evoked activities. Nat. Neurosci., *11*, 535-537.

43. Tan, A.Y., and Wehr, M. (2009). Balanced tone-evoked synaptic excitation and inhibition in mouse auditory cortex. Neuroscience *163*, 1302-1315.

44. Graupner, M., and Reyes, A.D. (2013). Synaptic input correlations leading to membrane potential decorrelation of spontaneous activity in cortex. J. Neurosci. *33*, 15075-15085.

45. Xue, M., Atallah, B.V., and Scanziani, M. (2014). Equalizing excitation-inhibition ratios across visual cortical neurons. Nature *511*, 596-600.

46. Larkum, M.E., Watanabe, S., Nakamura, T., Lasser-Ross, N., and Ross, W.N. (2003). Synaptically activated Ca2+ waves in layer 2/3 and layer 5 rat neocortical pyramidal neurons. J. Physiol. 549, 471-488.

47. Lee, K.F.H., Soares, C., Thiverge, J.-P., and Beique, J.-C. (2016). Correlated synaptic inputs drive dendritic calcium amplification and cooperative plasticity during clustered synapse development. Neuron *89*, 784-799.

48. Nishiyama, M., Hong, K., Mikoshiba, K., Poo, M.-M., and Kato, K. (2000). Calcium stores regulate the polarity and input specificity of synaptic modification. Nature 408, 584-588.

Acknowledgements:

We thank K. Kuchibhotla, M. Jin, E. Morina, D. Talos, and N. Zaika for comments, discussions, and technical assistance. This work was funded by grants from the Max Planck Society and a Career Award at the Scientific Interface from the Burroughs Wellcome Fund (to J.G.); and NIDCD (DC009635 and DC012557), NICHD (HD088411), a Sloan Research Fellowship, a Klingenstein Fellowship, and a Howard Hughes Medical Institute Faculty Scholarship (to R.C.F.).

Author Contributions:

All authors designed the studies and wrote the paper. R.E. Field, J.A. D'amour, and R. Tremblay performed the experiments and analyzed the data. C. Miehl and J. Gjorgjieva performed the modeling.